

# Numerical investigation of diffractive lens with the substrate shape influence included

B. DUBIK, J. MASAJADA, J. NOWAK, M. ZAJĄC

Institute of Physics, Technical University of Wrocław, Wybrzeże Wyspiańskiego 27, 50–370 Wrocław, Poland.

In this paper, a hybrid lens built up of thin (2-D) diffractive structure deposited on classic glass lens is considered. Such a lens can be treated as diffractive-refractive doublet. Its imaging quality depends on parameters of both parts: diffractive (radii of curvature of spherical waves generating diffraction microstructure and recording light wavelength) as well as refractive (radii of curvature of both surfaces, thickness and index refraction). The imaging quality is assessed via analysis of Point Spread Function (PSF) obtained by numerical calculation of respective diffraction integral. For the numerical evaluation of the PSF, it is assumed that diffraction occurs only on the 2-D diffractive microstructure; refractive part of hybrid lens influences only direction of light rays, along which the optical path is calculated. It is shown that the adopted model leads to correct results in numerical calculation of PSF for hybrid lenses recorded on surfaces of paraboloidal, spherical or elliptical shape.

## 1. Introduction

The standard method used to evaluate the quality of image formed by an optical element or system is based on the calculation of aberrations. Typically third order aberrations are considered. The wave aberration is used also for this purpose. Spot-diagram is a typical tool for image quality evaluation as well. All those methods are, in fact, based on the same approach, *i.e.*, on the ray tracing, and can be called "geometric" ones. A concept of light ray and calculation of its path (and direction) in transparent medium is an essence of all those methods [1]. An important physical phenomenon: light diffraction, which can influence strongly the imaging quality, is not taken into account. While calculating a spot-diagram, neither the interference of particular wave contributions nor diffraction on the boundary of an optical element is considered. Therefore, the distribution of points at which light rays intersect the plane of image detection does not necessarily reflect the real distribution of light energy in this plane. Moreover, the spot-diagram used to evaluate the image of a point object (aberration spot), by definition, does not give any information about complex light amplitude in the image. Therefore, it is impossible to estimate the image of multiple-point or extended objects (*e.g.*, three bar test or Ronchi ruling), especially in coherent or partially coherent illumination. Having this in mind, it seems that it is worth to develop an algorithm for calculation of the complex aberration spot using diffraction approach.

Such a "diffraction" method for calculation of aberration spot was proposed in [2] for holography and holographic lenses and then was used for analyzing the imaging by diffractive optical elements [3]. The method is based on numerical evaluation of the simplified diffraction integral. It is assumed that diffraction occurs on the 2-D microstructure of the optical element surface, and therefore the method is valid for thin optical elements, only.

However, every real optical element has finite thickness, and consequently two surfaces at least (complex optical systems can have many surfaces). Our particular interest is focused on the hybrid (diffractive-refractive) elements which have two surfaces. The 2-D diffractive microstructure is located on one of the surfaces, the other surface is a classic refractive one.

Simple extension of the above mentioned "diffraction" method of aberration spot evaluation to this case would need double integration (numerical calculation of diffraction integral over two surfaces). Analysis of more complex optical systems would need integration over even more surfaces. Consequently, the said method would be highly ineffective.

In the present paper, another algorithm of diffraction integral evaluation is presented. It needs only a single integration, so it can be successfully used for numerical modelling of image formation using the PC-type microcomputers.

## 2. Method of calculation

Complex light amplitude at a point  $P_i$  in the detection plane can be calculated from the simplified diffraction integral

$$U(P_i) = \int_{\Sigma} \exp(i\Delta\varphi) d\Sigma \quad (1)$$

where  $\Delta\varphi$  is a relative phase shift of the light wave travelling from the object point  $P_o$  to the image point  $P_i$  along a ray crossing the input pupil  $\Sigma$  at the point  $P_x$ , with respect to the phase shift between those points if calculated along the chief ray.

Two components are responsible for the phase shift  $\Delta\varphi$ . One, denoted by  $\Delta\varphi_1$ , is caused by the wave propagation from the point  $P_o$  to the point  $P_i$  through a lens (*comp.* Fig. 1) and equals:

$$\Delta\varphi_1 = \frac{-2\pi}{\lambda} (R_1 + nR'_2 + R''_2) \quad (2)$$

where:  $\lambda$  — light wavelength,  $n$  — refraction index of a lens material,  $R_1$ ,  $R'_2$ ,  $R''_2$  — distances shown in Fig. 1.

The second component of a phase shift,  $\Delta\varphi_2$ , is due to the light diffraction on the diffraction microstructure (surface  $S_1$ ) and is dependent on this microstructure. If the diffraction microstructure is generated as a recording of interference pattern of two spherical waves of radii  $R_\alpha$  and  $R_\beta$  (holographic lens), then

$$\Delta\varphi_2 = 2\pi\mu(R_\alpha - R_\beta) \quad (3)$$

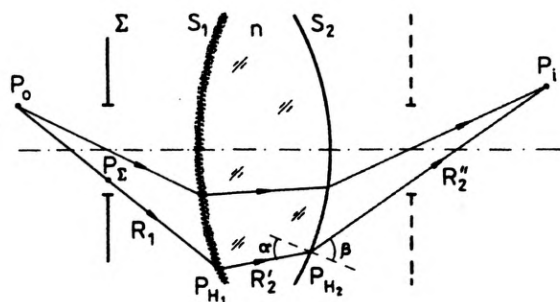


Fig. 1. Imaging geometry and notation

where:  $\mu = \lambda_o/\lambda$  is the ratio of the light wavelengths used when holo-lens recording and when imaging. Consequently, the aberration spot is calculated as

$$U(P_i) = \int_{\Sigma} \exp \left\{ \frac{-2\pi}{\lambda} (R_1 + nR_2' + R_2'') + \Delta\varphi_2 \right\} d\Sigma \quad (4)$$

where integration proceeds over the diffractive surface (the one with the microstructure). In other words, we assume that the light wave propagates according to the Fermat principle everywhere except the diffractive surface  $S_1$  (where microstructure is located). According to the Huygens principle, the direction of the light ray after passing this surface is not determined and can be chosen arbitrarily.

The main point of the present method lies in choosing the coordinates of points  $P_{H_1}$  and  $P_{H_2}$  (see Fig. 1). The location of point  $P_{H_1}$  depends on the location of object point  $P_o$  and the manner in which the input pupil  $\Sigma$  is divided (with points  $P_x$ ). The point  $P_{H_2}$  must be found in such a way that the ray  $P_{H_1} - P_{H_2} - P_i$  fulfils the law of refraction on the surface  $S_2$ . In practice, this can be done by dividing the output pupil instead of the input one and calculating the ray trace in the reversed direction (from  $P_i$  to  $P_{H_1}$ ).

The final formulae used for calculation of the aberration spot given by a hybrid lens designed as a classic lens with one (first) surface covered with a microstructure obtained as a holographic interference pattern are then:

$$U(P_i) = \frac{1}{n_x n_y} \sum_k \sum_l \exp \left[ \frac{-2\pi}{\lambda} (R_1 + nR_2' + R_2'') + \mu(R_\alpha - R_\beta) \right] \quad (5)$$

and

$$I(P_i) = U(P_i)U^*(P_i) \quad (6)$$

where:  $k, l$  - number the nodes of a grid into which the lens pupil is divided,  $n_x, n_y$  - number of those nodes.

The manner in which the lens pupil is divided depends on the overall shape and dimensions of this pupil and should assure its uniform filling out.

### 3. Numerical examples

To verify the algorithm described, two exemplary plano-convex hybrid lenses were investigated. The diffractive structure was recorded on the first, flat surface as a holo-lens with parameters:  $z_a = 100$  mm,  $z_b = -\infty$  and  $\lambda_0 = 632.8$  nm. The second surface was designed as hyperboloid with parameters:  $\rho = 100$  mm,  $\varepsilon = -1.25$  (lens No. 1 in the Table), or sphere of the same radius but with  $\varepsilon = 1$  (lens No. 2 in the Table). The lens thickness  $d = 3$  mm, the diameter of input pupil  $r = 6.66$  mm, the imaging light wavelength  $\lambda = 632.8$  nm, the index refraction of the lens material  $n = 1.5$ .

Table

Lens No.	Field angle	$I_{\max}$	$D_{08D}$	$D_{08D}$	$M_{2D}$	$M_{2D}$
1a	0	1	0	$1.0 \times 10^{-2}$	0	$5.7 \times 10^{-5}$
b	0.02	0.98	$4.5 \times 10^{-3}$	$1.1 \times 10^{-2}$	$1.2 \times 10^{-5}$	$6.0 \times 10^{-5}$
c	0.03	0.91	$1.1 \times 10^{-2}$	$1.3 \times 10^{-2}$	$6.2 \times 10^{-5}$	$7.7 \times 10^{-5}$
d	0.04	0.75	$1.9 \times 10^{-2}$	$1.9 \times 10^{-2}$	$2.0 \times 10^{-4}$	$1.0 \times 10^{-4}$
2a	0	0.98	$3.5 \times 10^{-3}$	$1.0 \times 10^{-2}$	$5.2 \times 10^{-6}$	$5.8 \times 10^{-5}$
b	0.02	0.97	$7.5 \times 10^{-3}$	$1.1 \times 10^{-2}$	$3.2 \times 10^{-5}$	$6.3 \times 10^{-5}$
c	0.03	0.89	$1.3 \times 10^{-2}$	$1.4 \times 10^{-2}$	$9.8 \times 10^{-5}$	$7.2 \times 10^{-5}$
d	0.04	0.72	$2.1 \times 10^{-2}$	$2.2 \times 10^{-2}$	$2.5 \times 10^{-4}$	$1.2 \times 10^{-4}$

It is well known that hyperboloidal refractive surface focuses perfectly light beams parallel to its axis. This property is exploited for designing the aberration free hybrid lens. A hybrid lens No. 1 will have such a property, if the object point is located on axis in object distance  $z_o = -100$  mm. The diffractive surface transforms the wave diverging from the object point  $P_o$  into parallel one which is then focused perfectly at the image point  $P_i$  ( $z_i = 203$  mm).

To estimate the influence of the way in which the lens pupil is divided, the aberration spot was calculated a number of times for different divisions [4]. It was then established that for uniform distribution of nodes of integration and radial symmetry, the number of  $N = 600$  points is quite enough and its increasing does not result in any noticeable change. The calculated 2-D light intensity distribution in the aberration free image is presented in Fig. 2a. This distribution is, within the computing error, equal to the theoretically expected  $|J_1(r)|^2$  function.

The following analysis was performed to compare the aberration spot calculated according to the presented algorithm and the typical spot diagram. In Figures 2a–d, meridional cross-sections of the aberration spots for different field angles are presented as well as the corresponding spot-diagrams (*nota bene* in the aberration free case, Fig. 2a, all geometry rays intersect at the same point and no spot diagram can be calculated, instead the 2-D aberration spot for this case is presented).

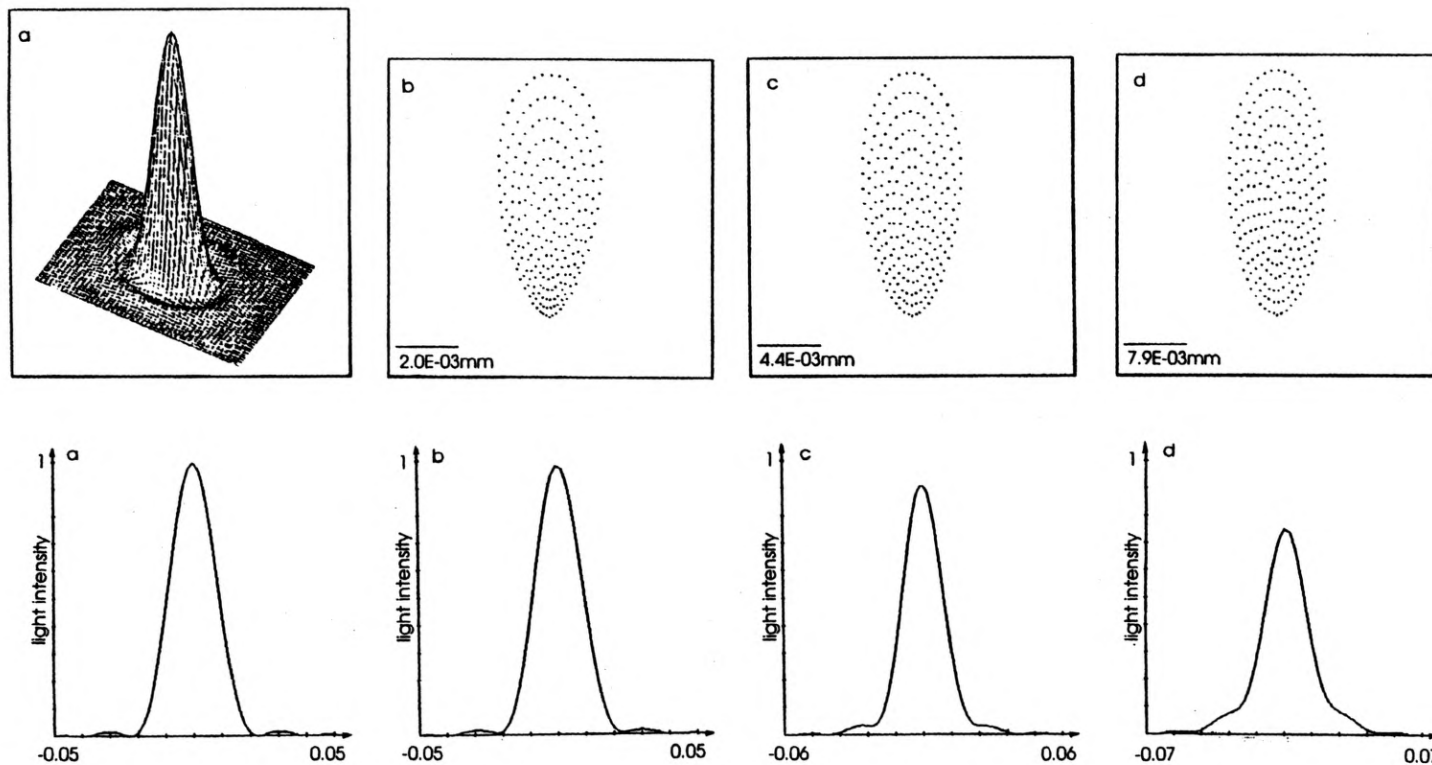


Fig. 2. Aberration spots for lens No. 1 and different fields angles  $\mu$ : a -  $\mu = 0$ , b -  $\mu = 0.02$ , c -  $\mu = 0.03$ , d -  $\mu = 0.04$ . Upper row - spot diagrams (for  $\mu = 0$ , a 3-D aberration spot), lower row - meridional cross-section of the light intensity distribution at the aberration spot

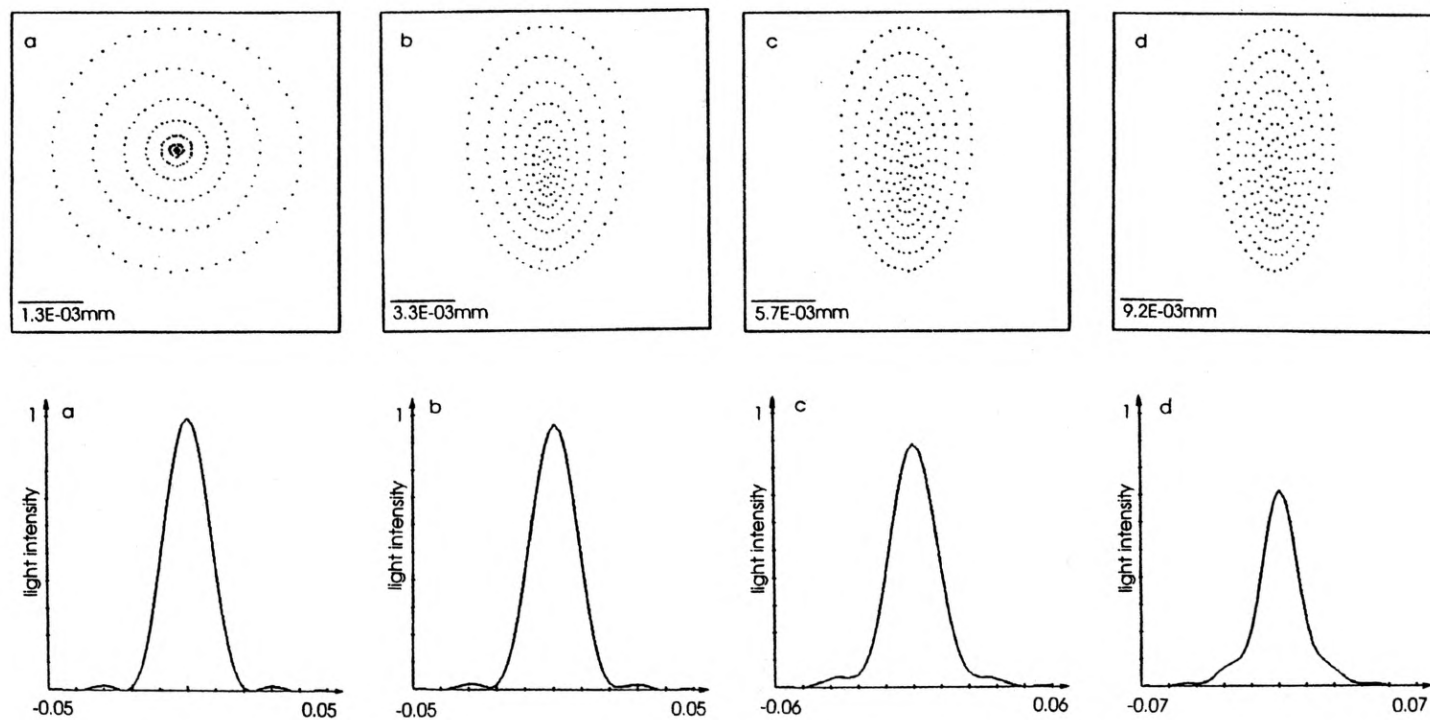


Fig. 3. Aberration spots for lens No. 2 and different field angles  $\mu$ : a —  $\mu = 0$ , b —  $\mu = 0.02$ , c —  $\mu = 0.03$ , d —  $\mu = 0.04$ . Upper row — spot-diagrams, lower row — meridional cross-section of the light intensity distribution at the aberration spot

presented). Some numerical parameters characterizing aberration spot are presented in the Table.  $I_{\max}$  denotes the maximum light intensity at the aberration spot (Strehl ratio) calculated with "diffraction" method.  $D_{0.8}$  stands for the diameter of a circle containing 80% of aberration spot total energy; subscript  $G$  denotes calculation based on the geometric spot-diagram, subscript  $D$  refers to the "diffraction" method.  $M_2$  is a second order moment of the light intensity distribution at the aberration spot (a measure of the spot "flatness"), and the subscripts  $G$  and  $D$  have the same meaning.

The last example calculated concerns the hybrid lens No. 2 which is no longer aberration free (even for the object on axis because of sphericity of the refractive surface). Figures 3a–d show meridional cross-sections of aberration spots calculated with "diffraction" method and geometrical calculated spot-diagrams similar to those for the lens No. 1. The analogous parameters characterizing aberration spot are presented in the Table as well.

#### 4. Conclusions

From the analysis of the presented graphs and numerical data, it can be seen that, to some extent, the results of both "diffraction" and geometrical methods are similar. General conclusions about the type of aberrations prevailing, overall shape and dimensions of aberration spot, *etc.*, are analogous. However, if the aberrations are small, an essential difference occurs. As it can be expected, geometrical method does not reflect any influence of the diffraction on the lens pupil and the calculated aberration spot is essentially smaller than in reality.

It seems that the "diffraction" method may be successfully used for analyzing the image quality of hybrid lens giving essentially more information than classic geometrical ray tracing method. Moreover, it can be easily generalized over the case of many refracting surfaces or non-homogeneous media (*e.g.*, gradient-index lenses).

#### References

- [1] WELFORD W. T., *Aberration of Optical Systems*, IOP Publ, London 1989.
- [2] NOWAK J. ZAJĄC M., *Opt. Acta* 12 (1983), 1749.
- [3] DUBIK B., MASAJADA J., NOWAK J., ZAJĄC M., *Opt. Eng.* 31 (1992), 478.
- [4] NOWAK J., *Hologram Aberrations in Image Quality Evaluation*, (in Polish), [Ed.] Technical University of Wrocław, Wrocław 1987.

Received October 18, 1993